Title
Ultrawideband photonic crystal fiber coupler for multiband optical imaging system.

Journal
Applied Optics, 49(10)

ISSN
1559-128X

Authors
Ryu, Seon Young
Choi, Hae Young
Choi, Eun Seo
et al.

Publication Date
2010-04-01

DOI
10.1364/ao.49.001986

Published in final edited form as:
Appl Opt. 2010 April 1; 49(10): 1986–1990.

Ultrawideband photonic crystal fiber coupler for multiband optical imaging system

Seon Young Ryu[1], **Hae Young Choi**[1], **Eun Seo Choi**[2], **Ivan Tomov**[3], **Zhongping Chen**[3], and **Byeong Ha Lee**[4,*]

[1]Division of Instrument Development, Korea Basic Science Institute, 113 Gwahangno, Yusung-gu, Daejeon 305-333, Korea

[2]Department of Physics, Chosun University, 375 Seosuk-dong, Dong-gu, Gwangju 501-759, Korea

[3]Beckman Laser Institute and Department of Biomedical Engineering, University of California, Irvine, California 92612, USA

[4]Department of Information and Communications, Gwangju Institute of Science and Technology, 261 Oryong-dong, Buk-gu, Gwangju 500-712, Korea

Abstract

We report a photonic crystal fiber (PCF) coupler having an ultrawide spectral bandwidth keeping single mode operation. The use of the PCF coupler in a fiber-based optical coherence tomography (OCT) system enables us to handle the wide spectral bands of various light sources, including superluminescent diodes (SLDs) at 1300 nm and 820 nm, Ti:sapphire lasers, and white-light sources. The multiband imaging performances of the PCF-based OCT system are demonstrated by obtaining dental images at 1300 nm and 820 nm with the same setup. In addition, we show that the PCF coupler could cover the spectrum over a one octave span and guide both the fundamental wave (1030 nm) and the second harmonic wave (515 nm) simultaneously.

1. Introduction

In biomedical application fields, optical imaging techniques have been widely studied due to their noninvasive imaging capability. Among them, optical coherence tomography (OCT) has provided highly sophisticated tomographic images of biological samples based on low coherence interferometery [1,2]. Therefore high axial resolution OCT images have been achieved by using broadband light sources such as white light [3], superluminescence diodes (SLDs), ultrafast pulse lasers, supercontinuum (SC) generated sources [4], or dual-band continuum generated sources [5]. Although many kinds of broadband light sources are available, there are some limitations in utilizing them for fiber-based OCT systems. In general, a conventional single mode fiber (SMF) has a cutoff wavelength, thus limiting the effective spectral bandwidth of the OCT system. Besides, it is difficult to fabricate a 2 × 2 fiber coupler using a conventional SMF, which can cover such a wide bandwidth [6]. These factors restrict available spectral bandwidth in the fiber-based high-resolution OCT system.

The broadband light sources have been employed not only for high resolution OCT systems but also for dual-band OCT systems for investigation of the relation between the probing depth and imaging quality in a dense tissue and for functional OCT imaging with

*Corresponding author: leebh@gist.ac.kr.

spectroscopic contrast [7,8]. In these systems, bulk optics were employed for simultaneous measurements at two different wavelength regions [7], and the use of bulk-type beam splitters is indispensable even for fiber based dual-band OCT systems [8] due to the absence of ultrawideband fiber-optic devices. By the same reason, two different couplers were used for the dual-band supercontinuum generated light source; one for each source [5]. In addition, recently, interest in the second harmonic (SH) OCT has increased due to its ability in enhancing the image contrast and identifying asymmetrically structured biological materials such as collagen [9–11]. The SH-OCT deals with two different colors that are spectrally separated by as much as one octave, which means that ultrawideband optical components are highly required in implementing the system. Therefore fiber and fiber devices that can support ultrabroadband are critical for fiber based ultrahigh resolution OCT or multiband OCT systems and realization of fiber based SH-OCT systems.

The utilization of photonic crystal fiber (PCF) and PCF couplers may overcome the limitation of conventional fiber and fiber coupler. It is well known that the PCF having a small filling factor has an endless single mode property [12]. Therefore the fiber coupler fabricated by the PCF is also single mode in a wide spectral bandwidth [13,14]. In this work, we propose an ultrawideband PCF coupler that can operate over a one octave wavelength range. Based on the PCF coupler, we have constructed a fiber-based ultrawideband OCT system. The feasibility of the ultrawideband OCT system is demonstrated by presenting the interferograms taken with various optical sources [superluminescent diodes (SLDs) at 820 nm and 1300 nm, a Ti:sapphire laser, and a white-light source] but with the same setup. The multiband OCT imaging performances were successfully obtained at 1300 nm and at 820 nm from a biological sample. In addition, we confirmed that the PCF coupler can guide both the fundamental (1030 nm) and the second harmonic waves (515 nm) generated from a nonlinear crystal to show the possibility of the realization of a fiber based SH-OCT system.

2. Fabrication and Properties of the PCF Coupler

For fabricating the PCF coupler, we exploited the conventional fused biconical tapered (FBT) method [13,15] using commercially available PCF (LMA-10, Crystal Fibre), which was composed with seven layers of air holes. The air hole separation, air hole diameter, and core diameter were about 7.21 μm, 2.88 μm, and 12 μm, respectively. This structure provides the single mode operation from 400 nm and large mode-field area suitable for high power delivery [16]. Two PCFs were twisted with each other and elongated while being heated with a hydrogen flame. During the elongation process, the pulling speed was kept as slow as possible, and the flame temperature was adjusted to be lower than that of the conventional fiber case by a few hundred degrees to keep the air hole structure. After heating and elongating, the coupler was packaged with a U-shape quartz rod to protect the fused region from unwanted bending or strain.

Figure 1(a) shows the input spectrum of a white light source and the transmission spectra measured at both output ports of the fabricated PCF coupler. A conventional white-light source (ANDO-AQ 4303B) was used, and the spectrum was measured with an optical spectrum analyzer (OSA). As we can easily estimate from Fig. 1(a), the insertion loss at a shorter wavelength region was higher than that at a longer wavelength region, and the splitting ratio had wavelength dependency. However, the PCF coupler shows relatively flattened coupling efficiency over an 800 nm spectral span. The total insertion loss of the coupler was measured as low as 3.5(±0.5) dB. To confirm the single mode operation of the PCF coupler, we have observed the mode-field pattern by a CCD camera after launching a 543.5 nm laser into the coupler. As can be seen in insets of Fig. 1(a), the mode-field shapes observed at both output ports showed a typical single mode characteristic, and it is

confirmed by a Gaussian fit as shown in Fig. 1(b). From these experimental results we can address that the proposed PCF coupler operates as an ultrawideband single-mode coupler.

3. Multiband Performances of the PCF Coupler

A PCF coupler-based time-domain OCT was implemented, and the axial point spread functions were measured with various light sources having different operating wavelengths: a 1300 nm centered SLD source (Kamelian; ~50 nm bandwidth), a 820 nm centered SLD source (INPHENIX; ~48 nm bandwidth), a Ti:sapphire (Ti : Al_2O_3) pulsed laser (~80 nm bandwidth corresponding to 10 fs FWHM pulse width) pumped with a 5.6 W solid-state laser (Verdi, 5.6 W at 532 nm), and a white-light source (ANDO-AQ 4303B). An InGaAs photodiode was used for the 1300 nm centered SLD source and the white-light source, while a fiber-pigtailed Si-based photodiode was used for the 820 nm centered SLD and the Ti:sapphire laser source.

Figure 2(a) shows the spectra of all light sources measured at an output port of the coupler, and the bottom figures show the corresponding single surface interferograms measured with the same setup but just with different light sources and corresponding detectors. The FWHMs of the interferograms, corresponding to the axial resolution of the OCT system, were measured 15 μm for the 1300 nm SLD [Fig 2(e)], 6 μm for the 820 nm SLD [Fig. 2(c)], and 4 μm for the Ti:sapphire pulsed laser [Fig. 2(b)]. These results are well matched with the theoretical ones except the axial resolution of 3 μm for the white-light source [Fig. 2(d)]. This discrepancy might be mainly caused by the limited spectral bandwidth of the detector. The asymmetry of the interferogram might be caused by the dispersion mismatch between the two arms of the interferometer or the dispersion of the PCF itself. To improve the utility of the PCF coupler in a high-resolution OCT system, fine dispersion balancing of the interferometer is required.

The biological imaging performance of the PCF coupler based OCT system at multispectral range was confirmed by taking OCT images with two SLD sources having different center wavelengths. The sensitivities at both 1300 nm and 820 nm were ~75 dB and ~73 dB, respectively. Figures 3(a) and 3(b) show the *in vitro* OCT images of a human tooth measured with the 1300 nm SLD and the 820 nm SLD, respectively. In the figures, we could clearly distinguish the enamel, dentin, and especially the dento-enamel junction. The area of each image was 6 mm × 3 mm in the transverse and the longitudinal directions. As expected, we can clearly see that the 1300 nm source is better than the 820 nm source for the dental OCT imaging, especially in its penetration depth.

4. Preliminary Study for the Fiber Based SH-OCT

Figure 4 presents the extended transmission spectrum of the same PCF coupler. In general, the OSA has a limited bandwidth, and its sensitivity becomes poor at short wavelengths. Although the coupling efficiency below 600 nm was poor, in the measured spectrum, and the spectral ripples are rather strong, the available spectral band of the PCF coupler ranged from 500 nm to more than 1400 nm, or >900 nm span. To check the possibility as a fiber-based SH-OCT system, the fundamental light beam from a high-power ytterbium-doped fiber laser (center wavelength, 1030 nm) [17] was directed to a BBO crystal ($\beta - BaB_2O_4$, 7 mm), and both the fundamental and the SH generated beams were launched to the input port of the PCF coupler as shown in Fig. 5. The back reflected fundamental and SH beams were split with a dichroic mirror at the detector arm of the interferometer and directed to a photodiode for the fundamental beam and to a photomultiplier tube (PMT) for the SH beam, respectively.

The SH wave, generated from BBO crystal, had a center wavelength at 515 nm and a 4 nm spectral bandwidth as shown with the spectrum of Fig. 6(a). The fundamental wave had a 1030 nm center wavelength and a 14 nm bandwidth as shown in Fig. 6(b). As demonstrated in Fig. 6(c), the interference fringe frequency measured by the PMT (bottom, thus the SH wave) was twice that recorded by the photodiode (top, thus the fundamental wave), which means that the PCF coupler guided both the fundamental wave and the SH wave successfully. Although a high insertion loss and a low coupling efficiency at a shorter wavelength range in the current system limit the capability of getting SH-OCT images from biological samples, we are sure that the PCF coupler has a great potential for the fiber-based SH-OCT system. The efforts to improve the performance of PCF devices for SH-OCT are under taken.

5. Conclusion

We have fabricated an ultrawideband PCF coupler that operated as a beam splitter, while keeping the single mode characteristic. Based on the PCF coupler, we have implemented an ultrawideband OCT system. With the same setup, the axial point spread functions of several light sources, having different center wavelengths and bandwidths, were measured. By using two SLD sources of 820 nm and 1300 nm, it was also demonstrated that the biological OCT imaging performance was well maintained without appreciable distortion. Furthermore, both the fundamental and the second harmonic waves were concurrently measured, which proved that the PCF coupler could cover the wide spectral range over one octave span. The spectral and modal features of the proposed PCF coupler might be suitable for implementing an ultrawideband or multiband fiber optic imaging system, including the fiber-based second harmonic OCT system.

Acknowledgments

This work was supported in part by a Korea Science and Engineering Foundation (KOSEF) grant funded by the Korea government (MEST) (No. R01-2007-000-20821-0), the KOSEF NCRC grant funded by MEST (No. R15-2008-006-02002-0), Korea, and research grants from the US National Institutes of Health (NIH) (EB-00293, NCI-91717, and RR-01192), US Air Force Office of Scientific Research (FA9550-04-1-0101), and the Beckman Laser Institute Endowment.

References

1. Huang D, Swanson EA, Lin CP, Schuman JS, Stinson WG, Chang W, Hee MR, Flotte T, Gregory K, Puliafito CA, Fujimoto JG. Optical coherence tomography. Science. 1991; 254:1178–1181. [PubMed: 1957169]
2. Fujimoto JG. Optical coherence tomography for ultrahigh resolution *in vivo* imaging. Nat. Biotechnol. 2003; 21:1361–1367. [PubMed: 14595364]
3. Ohmi M, Haruna M. Ultra-high resolution optical coherence tomography using a halogen lamp as the light source. Opt. Rev. 2003; 10:478–481.
4. Unterhuber A, Povazay B, Bizheva K, Hermann B, Sattmann H, Stingl A, Le T, Seefeld M, Menzel R, Preusser M, Budka H, Schubert Ch, Reitsamer H, Ahnelt PK, Morgan JE, Cowey A, Drexler W. Advances in broad bandwidth light sources for ultrahigh resolution optical coherence tomography. Phys. Med. Biol. 2004; 49:1235–1246. [PubMed: 15128201]
5. Aguirre AD, Nishizawa N, Fujimoto JG, Seitz W, Lederer M, Kopf D. Continuum generation in a novel photonic crystal fiber for ultrahigh resolution optical coherence tomography at 800 nm and 1300 nm. Opt. Express. 2006; 14:1145–1160. [PubMed: 19503436]
6. Wang Y, Zhao Y, Nelson JS, Chen Z. Ultra-high resolution optical coherence tomography by broadband continuum generation from a photonic crystal fiber. Opt. Lett. 2003; 28:182–184. [PubMed: 12656325]

7. Schmitt JM, Knuttel A, Yadlowsky M, Eckhaus MA. Optical-coherence tomography of a dense tissue: statistics of attenuation and backscattering. Phys. Med. Biol. 1994; 39:1705–1720. [PubMed: 15551540]

8. Kray S, Spöler F, Först M, Kurz H. High-resolution simultaneous dual-band spectral domain optical coherence tomography. Opt. Lett. 2009; 34:1970–1972. [PubMed: 19571969]

9. Jiang Y, Tomov I, Wang Y, Chen Z. Second-harmonic optical coherence tomography. Opt. Lett. 2004; 29:1090–1092. [PubMed: 15181995]

10. Sarunic MV, Applegate BE, Izatt JA. Spectral domain second-harmonic optical coherence tomography. Opt. Lett. 2005; 30:2391–2393. [PubMed: 16196329]

11. Su J, Tomov IV, Jiang Y, Chen Z. High-resolution frequency-domain second-harmonic optical coherence tomography. Appl. Opt. 2007; 46:1770–1775. [PubMed: 17356620]

12. Birks TA, Knight JC, St. J. Russell P. Endlessly single-mode photonic crystal fiber. Opt. Lett. 1997; 22:961–963. [PubMed: 18185719]

13. Lee BH, Eom JB, Kim JC, Moon DS, Paek UC. Photonic crystal fiber coupler. Opt. Lett. 2002; 27:812–814. [PubMed: 18007936]

14. Kim H, Kim JC, Paek UC, Lee BH. Tunable photonic crystal fiber coupler based on a side-polishing technique. Opt. Lett. 2004; 29:1194–1196. [PubMed: 15209244]

15. Ryu SY, Choi HY, Na J, Choi ES, Yang GH, Lee BH. Optical coherence tomography implemented by photonic crystal fiber. Opt. Quantum Electron. 2005; 37:1191.

16. Nielsen MD, Mortensen NA, Folkenberg JR. Reduced microdeformation attenuation in large-mode-area photonic crystal fibers for visible applications. Opt. Lett. 2003; 28:1645–1647. [PubMed: 13677523]

17. Lim H, Jiang Y, Wang Y, Huang Y, Chen Z. Ultrahigh-resolution optical coherence tomography with a fiber laser source at 1 μm. Opt. Lett. 2005; 30:1171–1173. [PubMed: 15945143]

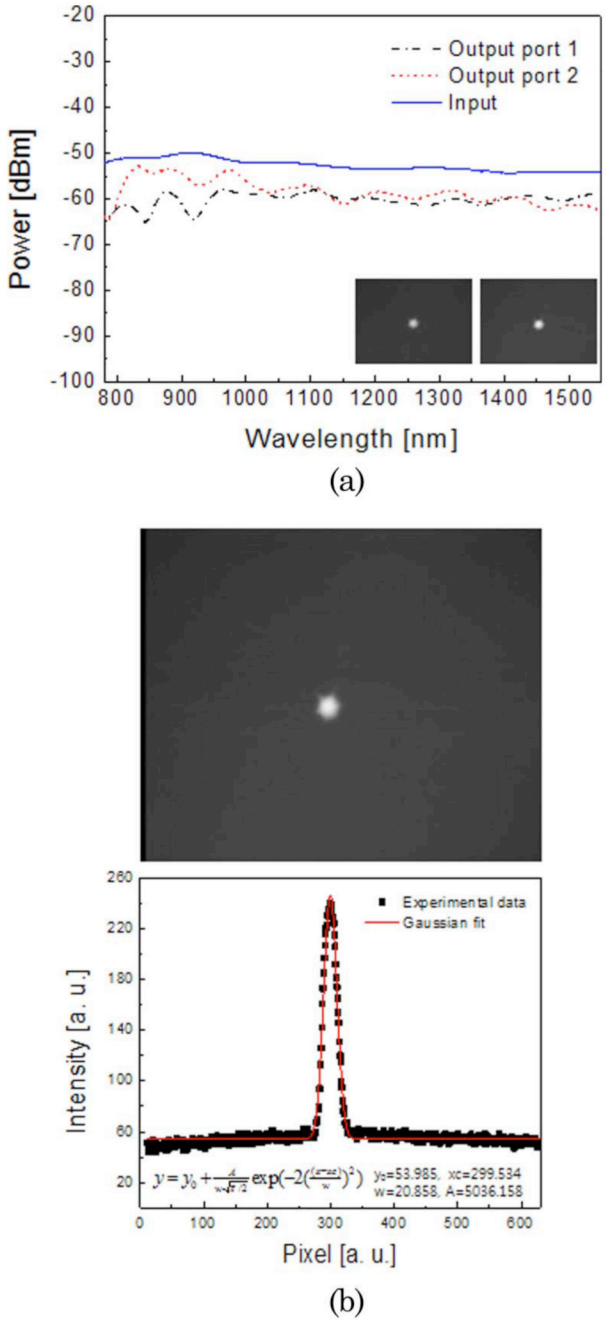

Fig. 1.

(Color online) (a) Transmission spectrum of an input white-light source and the transmission spectra measured at both output ports of the fabricated PCF coupler. The inset pictures are mode-field patterns at both ports that are taken with a CCD camera at a 543.5 nm wavelength. (b) The mode-field pattern measured at output port 1 and one of the cross sections with a corresponding Gaussian fit curve.

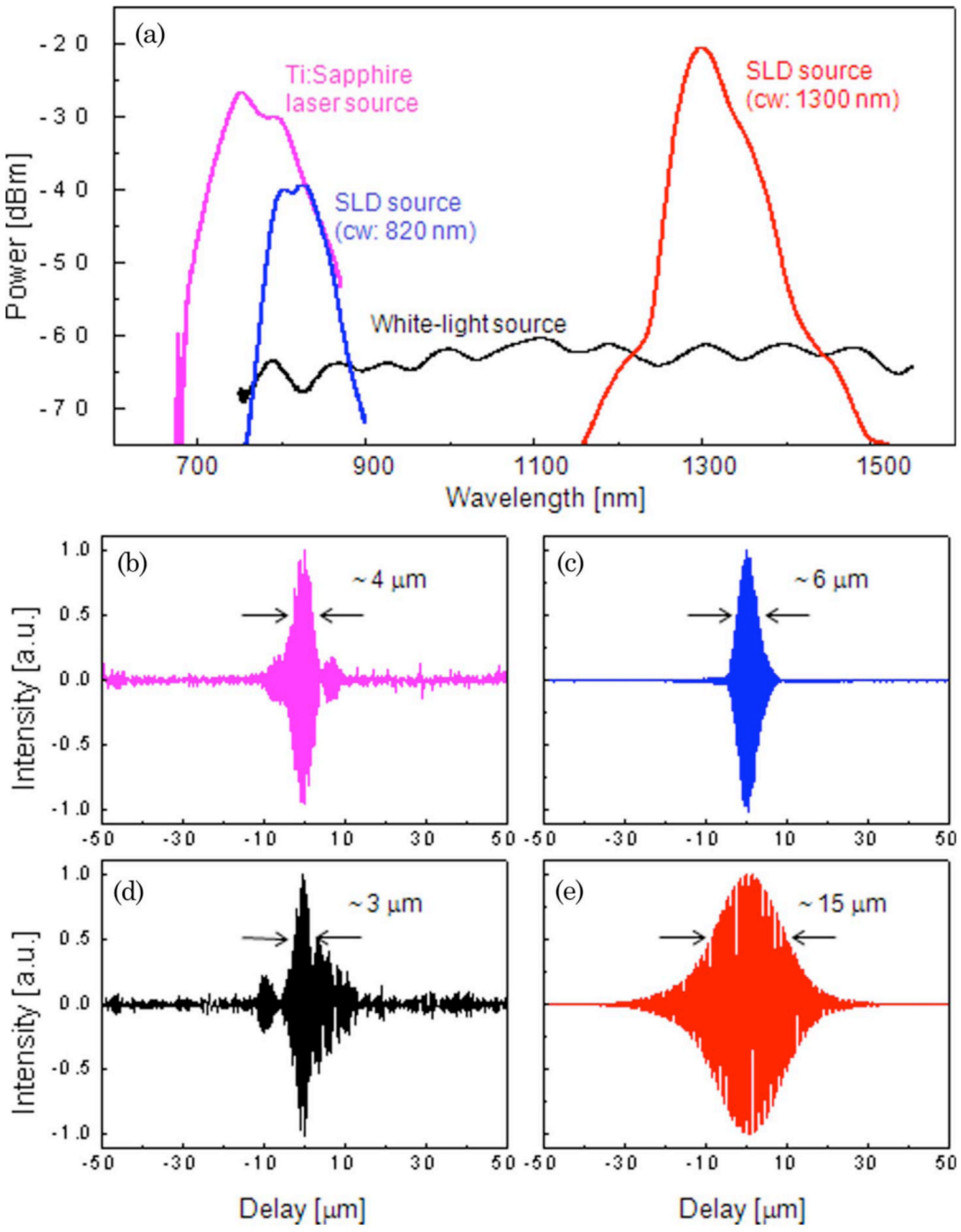

Fig. 2.

(Color online) (a) Transmission spectra and the corresponding interferograms with various light sources: (b) for a Ti:sapphire laser source (cw; 760 nm; bw; 80 nm), (c) for a SLD source (cw; 820 nm; bw; 48 nm), (d) for a white light source, and (e) for a SLD source (cw; 1300 nm; bw; 50 nm); cw is center wavelength, and bw is bandwidth.

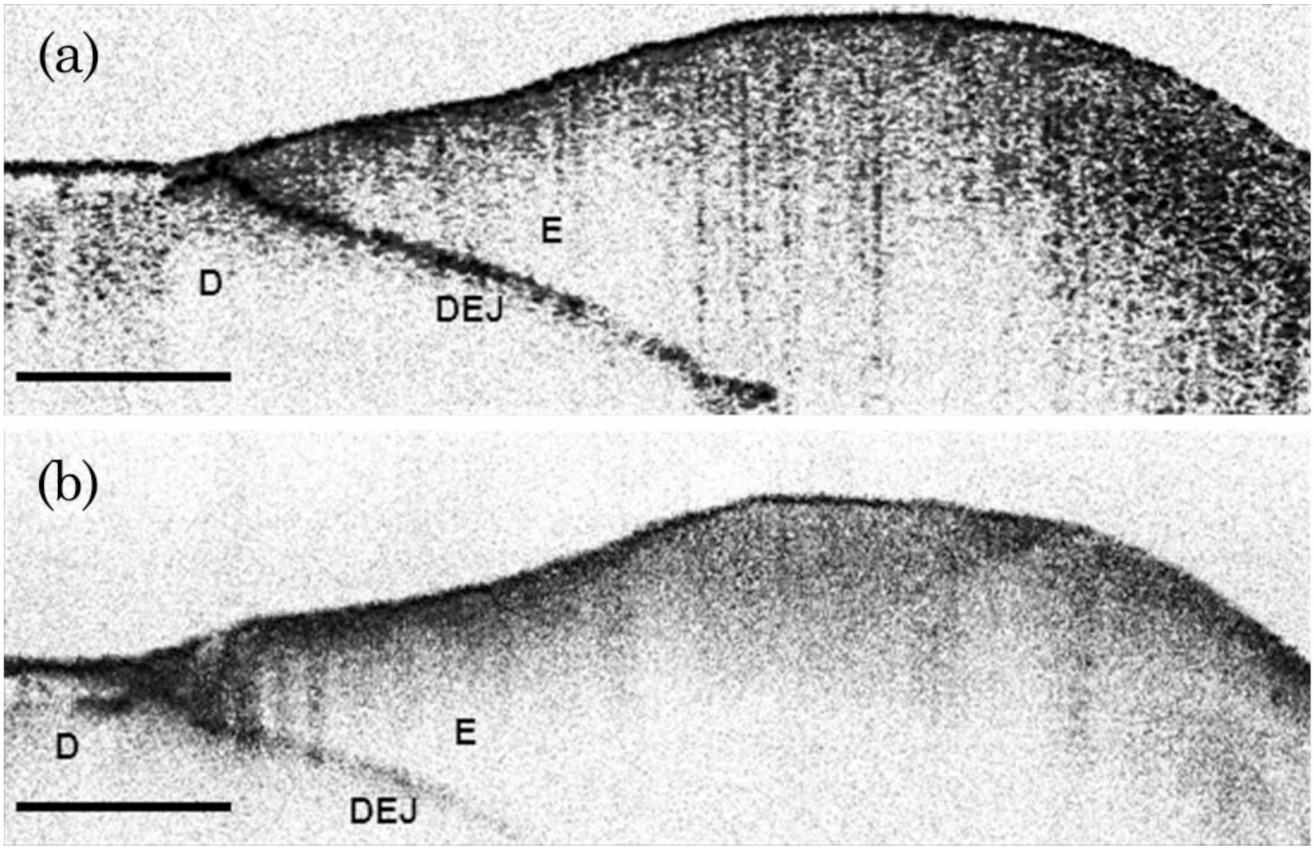

Fig. 3.
OCT images of a human tooth obtained with the OCT system based on the proposed ultrawideband PCF coupler but with SLD sources having different center wavelengths: (a) 1300 nm and (b) 820 nm (D, dentin; E, enamel, DEJ, dento-enamel junction). Scale bar is 1 mm.

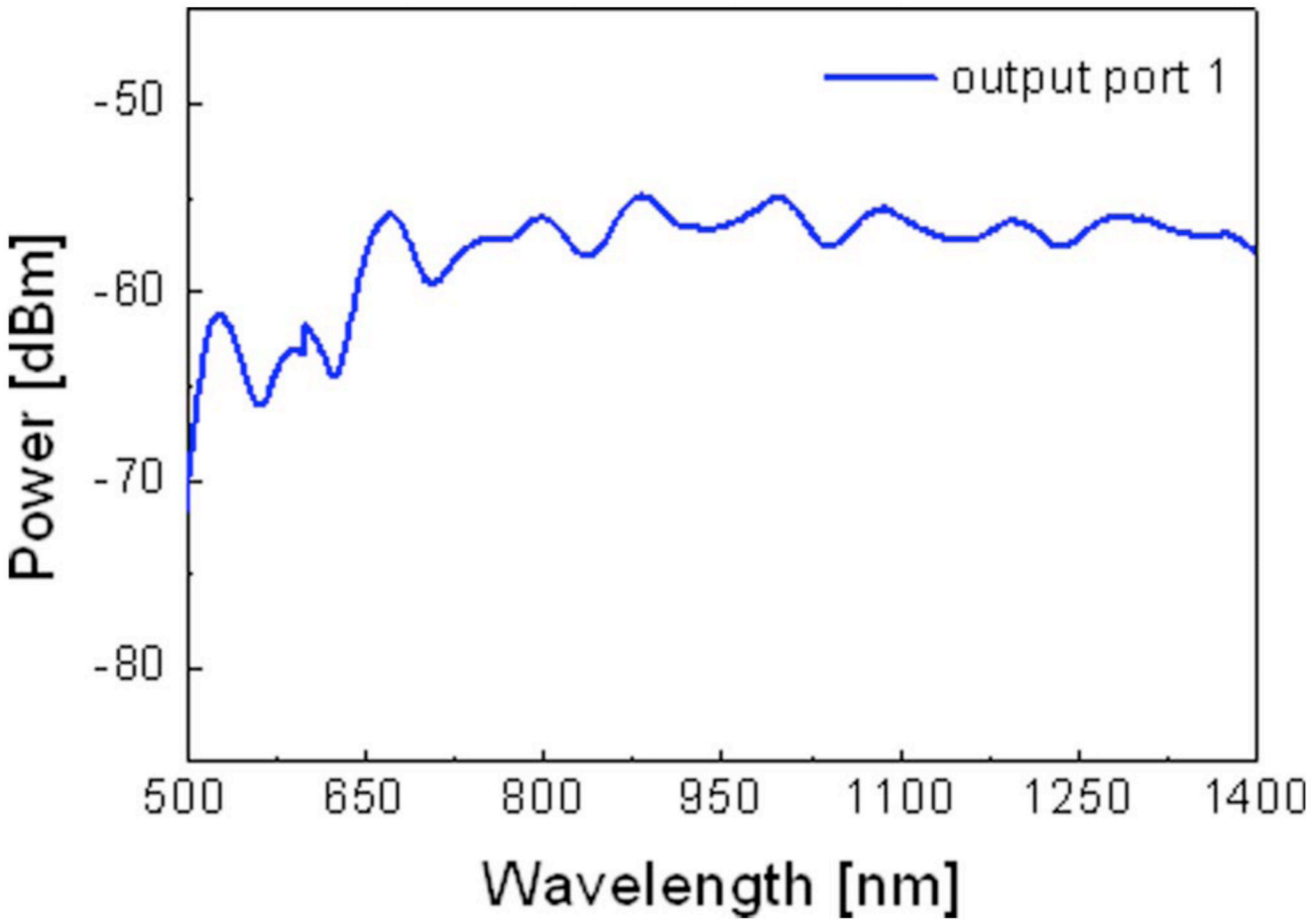

Fig. 4.
(Color online) Extended transmission spectrum at output port 1 of the PCF coupler. The available spectral band of the PCF coupler ranged from 500 nm to more than 1400 nm.

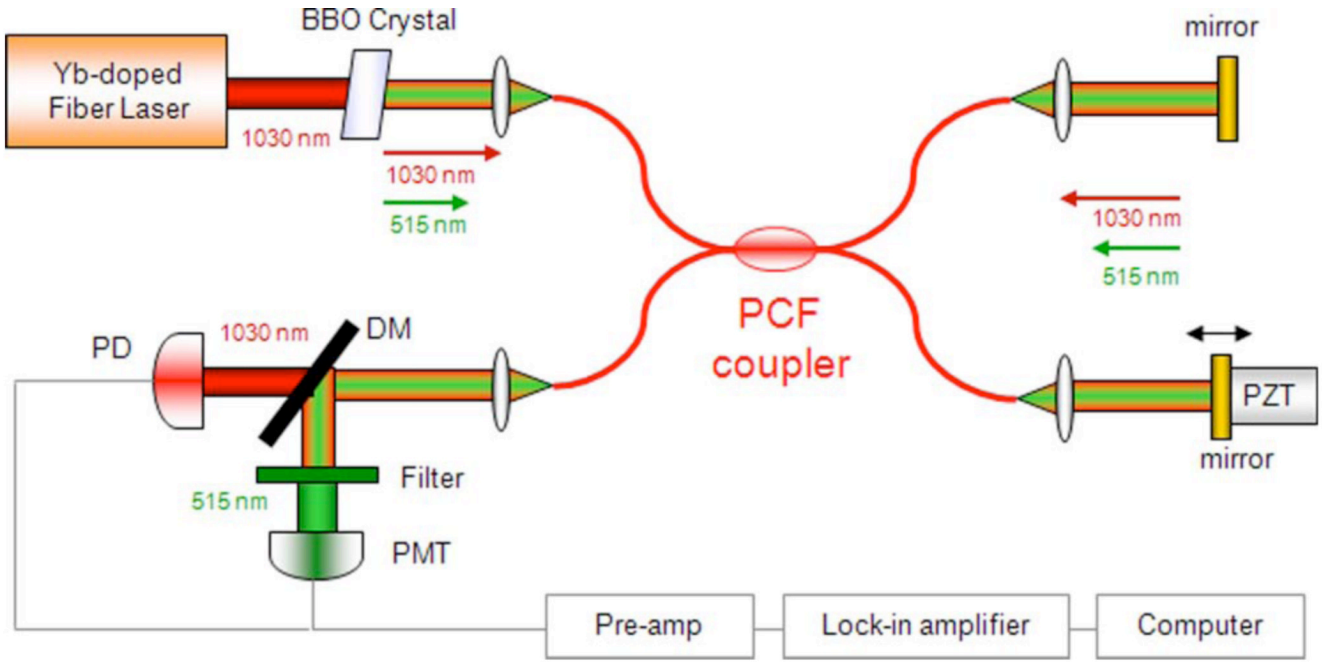

Fig. 5.

(Color online) PCF coupler based interferometer for measurements of both fundamental and SH waves. A high power Yb-doped fiber laser and BBO crystal ($\beta - BaB_2O_4$) are used for generation of SH waves. (DM, dichroic mirror; PD, photodetector; and PMT, photomultiplier tube).

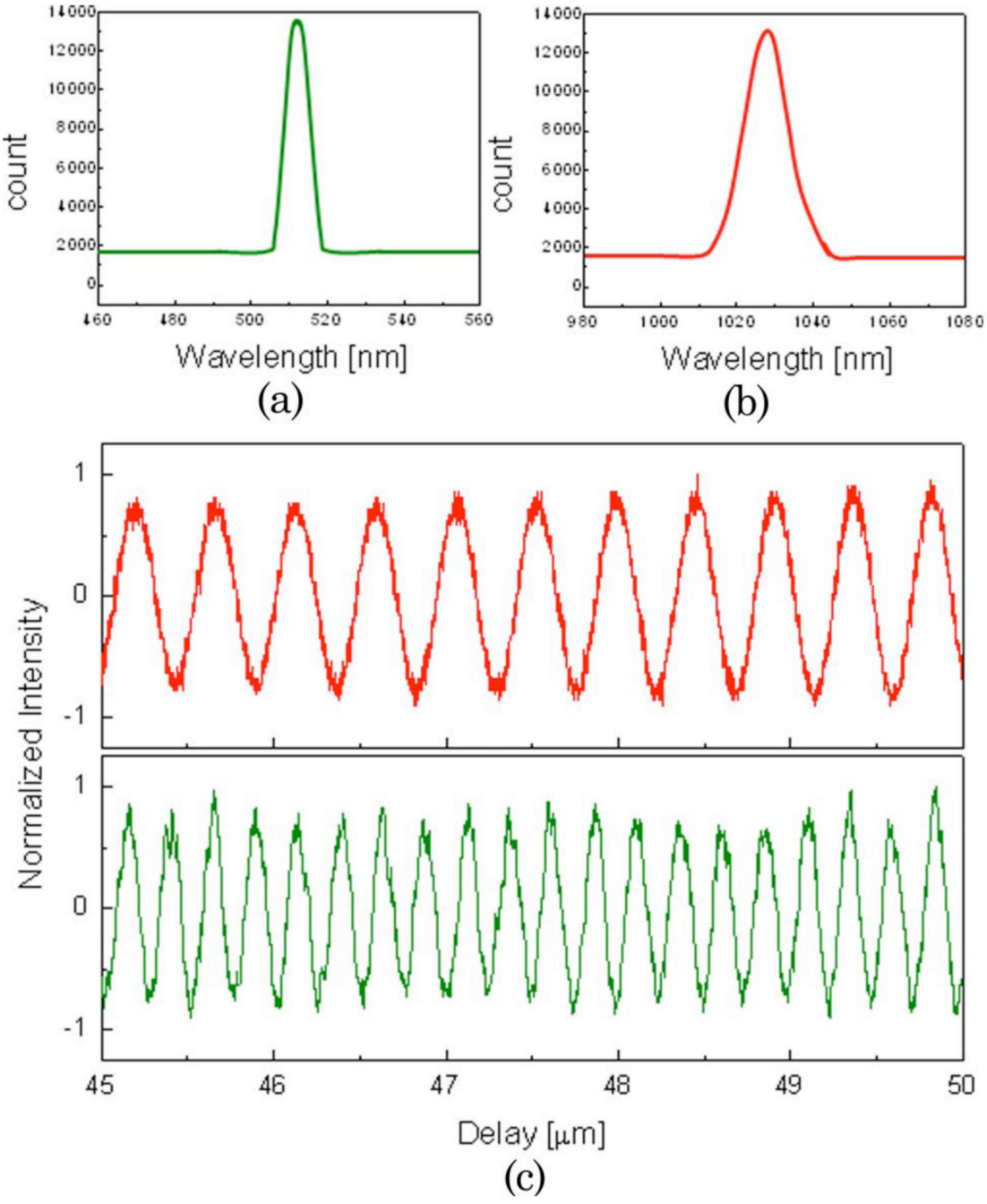

Fig. 6.
(Color online) Output spectra of (a) the fundamental wave and (b) the SH wave; (c) enlarged interference fringes from the fundamental wave (top) and the SH wave (bottom).